Macromolecules

pubs.acs.org/Macromolecules Article

Polyzwitterions with LCST Side Chains: Tunable Self-Assembly

Tao Jiang, Vladimir Aseyev, Jukka Niskanen, Sami Hietala, Qilu Zhang,* and Heikki Tenhu*

Cite This: *Macromolecules* 2020, 53, 8267−8275

Read Online

ACCESS | Metrics & More | Article Recommendations | Supporting Information

ABSTRACT: Manipulation of self-assembly behavior of copolymers via environmental change is attractive in the fabrication of smart polymeric materials. We present tunable self-assembly behavior of graft copolymers, poly(sulfobetaine methacrylate)-*graft*-poly[oligo(ethylene glycol) methyl ether methacrylate)-*co*-di(ethylene glycol) methyl ether methacrylate] (PSBM-*g*-P(OEGMA-*co*-DEGMA)). Upon heating the aqueous solutions, the graft copolymers undergo a transition from micelles with PSBM cores to unimers (i.e., individual macromolecules) and then to reversed micelles with P(OEGMA-*co*-DEGMA) cores, thus demonstrating the tunability of the self-assembling through temperature change. In the presence of salt the temperature response of PSBM is eliminated, and the structure of the micelles with the P(OEGMA-*co*-DEGMA) core changes. Moreover, for the graft copolymer with long side chains, micelles with aggregation number ∼ 2 were formed with a PSBM core at low temperature, which is ascribed to the steric effect of the P(OEGMA-*co*-DEGMA) shell.

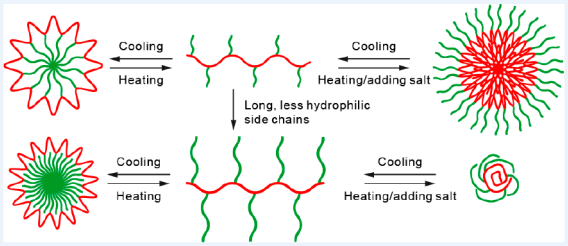

INTRODUCTION

Stimuli-induced shape change of ordered structures plays a key role in living and many nonliving systems. Proteins are one of the most sophisticated natural polymers that can respond to variations in the environment and change their 3D structures to perform highly specific functions, for example, enzymatic catalysis or switching of permeation (ion channels). Synthetic polymers have been developed to mimic this behavior, and this has led to several types of smart polymeric materials.[1−4] Stimuli-responsive polymers that can change the self-assembly structures upon environmental change have been mostly mentioned and are used for example for cargo release or mechanical actuation.[5−8]

Double-responsive copolymers with opposite responses are stimuli-responsive polymers that can switch their self-assembly from one structure to a reversed one upon minor environmental change.[9−24] Historically, these polymers have been called "schizophrenic", but we call them "oppositely responsive" ones. Such copolymers usually contain two blocks that can switch between hydrophilic and hydrophobic properties in response to various stimuli such as pH,[9,10,13,18,20−24] temperature,[10,11,17,19,21−23] ionic strength,[9,14] light,[13] CO_2,[12] and so on. Within the above-mentioned triggers, temperature-induced phase transition is the most attractive one since only a small change in temperature is required, while no salts, acids, or bases are needed to be added to the solution.[25−29] Laschewsky et al. reported the first oppositely thermoresponsive linear diblock copolymer that was composed of a poly(*N*-isopropylacrylamide) (PNIPAM) block and a poly(3-[*N*-(3-methacrylamidopropyl)-*N*,*N*-dimethyl]-ammoniopropanesulfonate) (PSPP) block showing the lower critical solution temperature (LCST) and the upper critical solution temperature (UCST) behavior, respectively.[17,19,30−32] Later on, we developed a triple thermoresponsive linear diblock copolymer consisting of a poly(oligo ethylene glycol methyl ether methacrylate) (POEGMA, LCST) block and a poly(dimethylaminoethyl methacrylate) (PDMAEMA, both LCST and UCST[33,34]) block.[11] The obtained copolymer exhibited transition from self-organized multimolecular associates, the exact architecture of which was not defined, via unimers (individual polymer chains) to reversed micelles (or vesicles) as the temperature increased and finally collapsed into a precipitated state at an even higher temperature. These switchable self-assembly structures are promising for controlled drug release, gene delivery, nanocatalysis, and so forth.[26,35−38]

In contrast to a number of oppositely responsive linear copolymers with diverse stimuli-responsive and self-assembling behaviors, nonlinear block copolymers (such as polysulfobetaine based graft copolymers) with oppositely responsive behavior have not yet been reported. Stimuli-responsive nonlinear copolymers studied previously differ from those of linear ones.[39−43] Thus, construction of nonlinear topologies and the stimuli-responsive and self-assembling behavior of nonlinear copolymers remains to be investigated. In particular, graft copolymers are of great interest due to their confined and compact structures[44−48] as well as their special self-assembling behavior in dilute solutions.[49−54] For instance, graft copoly-

Received: July 23, 2020
Revised: September 5, 2020
Published: September 17, 2020

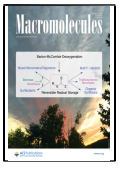

https://dx.doi.org/10.1021/acs.macromol.0c01708
Macromolecules 2020, 53, 8267−8275

Table 1. Parameters for Syntheses and Characterization of the Copolymers

	feed ratio							
	S70	OEGMA	DEGMA	conversion of side chain polymerization (%)	DP of side chain[a]	DP of side chain[b]	M_n[c] (kDa)	$Đ$[c]
S70							180	1.9
S70-*g*-O25D25	1[d]	35	35	70	49	50	248	2.9
S70-*g*-O70D280	1[d]	100	400	69	347	353	616	3.2

[a]Calculated with the conversion of the grafting polymerization by using ^{1}H NMR. [b]Calculated from the ratio of the *f* and *i* peak areas of the ^{1}H NMR spectra shown in Figure 1. [c]Estimated using AF4. [d]The molar ratio of bromine (Br) moieties.

mers with hydrophilic side arms and hydrophobic backbones have significantly lower aggregation number of the self-assembled micelles than those formed from linear copolymers.[49,50,52] Even unimolecular micelles can be formed when the hydrophobic backbone collapses in an unfavorable solvent and is shielded from other molecules by the surrounding hydrophilic side chains.[55−58]

We report the synthesis and self-assembling behavior of oppositely responsive graft copolymers, which form well-defined aggregates, unimers (soluble polymer chains), and reversed aggregates solely triggered by a temperature change. Such a schizophrenic property can be well tuned by varying the structure of the graft copolymers and the presence of salt. The obtained self-assembly structures are investigated by light scattering, which reveals the formation of conventional micelles, micelles with pores, and unimolecular reverse micelles depending on the structure of the graft copolymers and the environment.

EXPERIMENTAL SECTION

Materials. All chemicals and solvents are commercially available and were used as received unless otherwise stated. Sulfobetaine methacrylate monomer (SBM, also named [2-(methacryloyloxy)-ethyl]dimethyl-(3-sulfopropyl)ammonium hydroxide, Sigma-Aldrich) was purified by precipitation of its methanol solution against diethyl ether twice, followed by drying under reduced pressure at room temperature. The purified monomer was stored in a fridge before use. Oligo(ethylene glycol) methyl ether methacrylate (OEGMA, Sigma-Aldrich, averaged molar mass 300 Da) and di(ethylene glycol) methyl ether methacrylate (DEGMA, Sigma-Aldrich) were purified by passing through neutral alumina column chromatography to remove the inhibitors and were stored in a fridge before use. Copper metal chips were washed, successively, with dilute sulfuric acid and water (many times) to remove oxidized copper from surface. The cleaned copper chips were stored under nitrogen gas.

Synthesis of Inimer BIHPM. *Inimer 2-(2-Bromoisobutyryloxy)-3-hydroxypropyl Methacrylate (BIHPM) Synthesized in Two Steps.* First, glycidyl methacrylate was dissolved in a mixture of 1 N H_2SO_4 and THF with 50/50 (v/v). The solution was allowed to react for 2 h under continuous stirring at room temperature. The crude product was then extracted four times with dichloromethane (DCM). The organic phases were combined, concentrated, and dried over magnesium sulfate. The product, glyceryl methacrylate, was purified by silica column eluted with DCM followed by evaporation of the solvent.

Next, α-bromoisobutyryl bromide (4.94 mL, 0.04 mol) in DCM (20 mL) was added dropwise into a solution of glyceryl methacrylate (6.73 g, 0.042 mol) and triethylamine (5.58 mL, 0.04 mol) in dichloromethane (DCM, 500 mL), under vigorous stirring in an ice water bath. After 20 h, the solution was washed twice with saturated aqueous sodium bicarbonate solution and dried with magnesium sulfate. The mixture was purified by column chromatography using silica gel as stationary phase and cyclohexane/diethyl ether (50/50, vol/vol) solvent mixture as eluent. After evaporation, two isomers were collected, 2-(2-bromoisobutyryloxy)-3-hydroxypropyl methacrylate and 3-(2-bromoisobutyryloxy)-2-hydroxypropyl methacrylate, with 3-(2-bromoisobutyryloxy)-2-hydroxypropyl methacrylate (BIHPM) as main product. In total, 6.19 g of product was obtained (47.7% yield). ^{1}H NMR (500 MHz, $CDCl_3$): δ 6.18, 5.61 s (CH_2CCH_3); δ 4.15−4.35 m ($OCH_2CH(OH)CH_2O$ or OCH_2CHCH_2OH); δ 2.7 s (*OH*); δ 1.8−2.0 m (CH_2CCH_3, $C(CH_3)_2Br$).

Preparation of Poly(sulfobetaine methacrylate) (PSBM) Macroinitiator. The PSBM macroinitiator was synthesized by copolymerization of SBM and BIHPM via free radical polymerization. SBM, BIHPM, and 4,4′-azobis(4-cyanovaleric acid) (ACVA) were dissolved in a solvent mixture of water (0.5 M NaCl) and DMF. The solution was then purged with nitrogen for 30 min to remove oxygen. Polymerization was initiated by placing the solution vessel into a preheated oil bath at 70 °C. The solution was allowed to react for at least 18 h. The solution was then cooled to room temperature, and the polymer was precipitated into ethanol. The polymer was dissolved in 0.1 M NaCl and dialyzed first in saline water and then in distilled water. The polymer was recovered by lyophilization and characterized by ^{1}H NMR and size exclusion chromatography (SEC).

Synthesis of PSBM-g-P(OEGMA-co-DEGMA). In a typical synthesis of S70-*g*-O70D280, PSBM macroinitiator (100.2 mg) was first dissolved in 15 mL of 0.5 M NaCl solution with vigorous stirring. 150.0 mg of OEGMA and 376.4 mg of DEGMA were then added dropwise to the solution to avoid inhomogeneous distribution of the components of the mixture. Then, 0.17 mL of Cu(II)Cl_2 stock solution (0.2 mg/mL), 0.23 mL of tris[2-(dimethylamino)ethyl]-amine (Me_6TREN) stock solution (1.0 mg/mL), and 0.2 mL of DMF (internal standard for the determination of monomer conversions by ^{1}H NMR) were added. The solution was bubbled with nitrogen gas for 30 min to remove oxygen. One spoonful of copper metal chips was added to the solution to start the polymerization process at room temperature. The reaction was quenched by exposure to air after 25 min, after which the liquid part of the mixture was collected and purified via dialysis against, successively, saline and distilled water followed by lyophilization to obtain pure product. The graft copolymer with shorter and more hydrophilic O(D)EGMA side chains, S70-*g*-O25D25, was synthesized in a similar manner, with a feed ratio of OEGMA and DEGMA described in Table 1. The resulted copolymers were characterized by ^{1}H NMR and asymmetric flow field flow fractionation (AF4).

Characterization. ^{1}H NMR spectra were collected by using a Bruker Avance III 500 MHz spectrometer. The chemical shifts presented are in parts per million downfield from the internal TMS standard. For the ^{1}H NMR spectra of the polymer solutions (1 mg/mL in neat D_2O or 0.1 M NaCl in D_2O) the temperature was varied from 5 to 50 °C with an interval of 5 °C. For each temperature, the sample was allowed to stabilize for 10 min prior to measurement.

Asymmetric flow field-flow fractionation (AF4) was performed on a Wyatt Eclipse separation system equipped with UV (Agilent 1230 infinity, Agilent), refractive index (Optilab rex, 633 nm, Wyatt), and multiangle light scattering (MALLS) (Dawn Heleos-II, 663 nm, Wyatt) detectors. The samples were delivered with an Agilent pump. A regenerated cellulose membrane from Millipore with a molar mass cutoff of 10 kDa was used as an accumulation wall. A 50 mM $NaNO_3$/3 mM NaN_3 buffer solution was used as the eluent. The focus flow was set to be 1.5 mL/min for 3 min after injection of 3 μL (1 mg/mL) of the polymer samples with 0.2 mL/min. The cross-flow was first set as 3 mL/min for 5 min after the focusing period and been decreased under exponential decay to 0 mL/min within 30 min. For

https://dx.doi.org/10.1021/acs.macromol.0c01708
Macromolecules 2020, 53, 8267−8275

Scheme 1. Synthesis Route of Double-Responsive Graft Copolymers

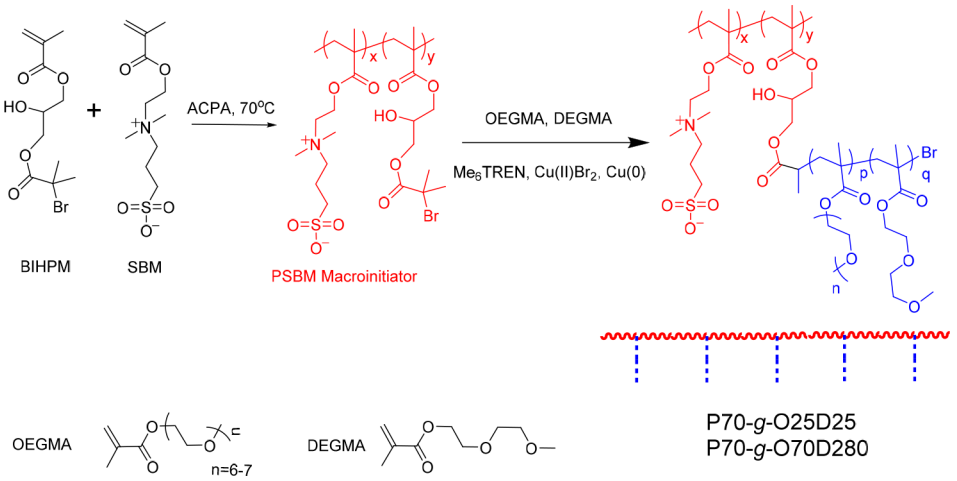

calculation of the molar mass by MALLS, a Debye plot with the Zimm method was used. Refractive index increments, dn/dc, were measured with an Optilab Rex detector and analyzed by using Astra software from Wyatt.

Dynamic light scattering (DLS) measurements were performed by using a Zetasizer Nano instrument from Malvern equipped with a He−Ne laser (633 nm wavelength) and a detector at a 173° backscattering angle. Disposable polystyrene square cuvettes were used, and all samples of a 1 mg/mL concentration were filtered with disposable 0.45 μm PALL ACRODISC syringe filter units prior to use. An apparent translational diffusion coefficient (D) was obtained by using a multiexponential inverse Laplace transfer algorithm and translated to an intensity-weighted apparent hydrodynamic radius (R_h) distribution through the Stokes−Einstein relation:

$$D = \frac{\Gamma}{q^2} = \frac{k_B T}{6\pi\eta R_h} \quad (1)$$

where k_B is the Boltzmann constant, T is the absolute temperature, and η is the viscosity of the solvent, $q = 4\pi n \sin(\theta/2)/\lambda$ is the scattering vector, λ is the laser wavelength, n is the refractive index of the solvent, and θ is the scattering angle. The volume-weighted R_h distribution was then calculated by assuming the detected nanoparticles (individual soluble polymer chains) are spherical. For each temperature, the sample was allowed to stabilize for at least ΔT min (ΔT is the temperature interval for heating or cooling) before the measurement.

A Brookhaven Instruments goniometer (BIC-200SM), a BIC-Turbo-Corr digital pseudo-cross-correlator, and a BIC-CrossCorr detector equipped with two BIC-DS1 detectors were set up to perform static (SLS) and dynamic (DLS) light scattering in the range of scattering angles of $30° < \theta < 150°$. The concentration of the polymer solutions was 1 mg/mL unless otherwise stated, which was regarded as dilute solution (i.e., no significant effect of concentration on the measured value of R_h). The decay rate (Γ) from the second-order cumulant fit versus the square of the scattering vector (q^2) was plotted and fitted with a linear dependence through the origin. The slope value was taken as the diffusion coefficient D, and the R_h values were calculated accordingly. The apparent weight-averaged molar mass (M_w) and radius of gyration (R_g) of the nanoparticles were estimated by the Zimm approach:

$$\frac{Kc}{R_\theta} = \frac{1}{M_w}\left(1 + \frac{R_g^2 q^2}{3}\right) \quad (2)$$

where K, c, R_θ, and M_w are the optical constant, polymer concentration, intensity of the scattered light expressed as the excess Rayleigh ratio of scattering particles over solvent, and the molar mass, respectively. The aggregation number was estimated as $M_{w,agg}/M_{w,unim}$, where $M_{w,agg}$ and $M_{w,unim}$ refer to the apparent weight-average molecular weight of the aggregate and the individual polymer chain, respectively.

RESULTS AND DISCUSSION

Two graft copolymers with different side-chain lengths were synthesized via a "grafting from" strategy (Scheme 1). The backbone of the graft copolymer was prepared via free radical copolymerization of sulfobetaine methacrylate (SBM) and a bromo-functionalized comonomer, BIHPM (a mixture of 2-(2-bromoisobutyryloxy)-3-hydroxypropyl methacrylate and 3-(2-bromoisobutyryloxy)-2-hydroxypropyl methacrylate; see the Experimental Section) with a SBM:BIHPM monomer ratio of 70 to 1 (Table 1). The resulted polymer, polySBM (PSBM), with BIHPM units randomly distributed along the chain was then used to initiate the polymerization of the side chains. A typical atom transfer radical polymerization (ATRP) procedure mediated by Cu(I) was the first trial for the grafting of PSBM. However, phase separation of the PSBM from solution (in aqueous solution with either 0.1 or 0.5 M NaCl) took place when Cu(I) was added as indicated by solution clouding. Although the reason for the phase separation yet is not clear, the electrostatic interaction between Cu(I) or Cu(II) cations and sulfonic anions in SBM is suspected. As an alternative, Cu(0)-mediated polymerization[59−61] was performed since it allows the use of a trace amount of Cu(II) instead of Cu(I) cations. No precipitation was observed after the addition of $Cu(II)Br_2$ and during the polymerization process. Two monomers, oligo(ethylene glycol) methyl ether methacrylate (OEGMA, with molar mass 300) and di(ethylene glycol) methyl ether methacrylate (DEGMA), were utilized as comonomers for the polymerization of side chains to obtain a tunable LCST behavior.[62] The monomer conversions for side-chain polymerizations were determined by monitoring ^{1}H NMR signals of vinyl protons with DMF as an internal standard at time zero and the end of polymerization, as shown in Table 1. It is noted that the conversions of monomers (for side-chain polymerization) were kept below 80% to suppress possible inter- and intrachain cross-linking which occurs frequently in the synthesis of graft polymers via "grafting from" strategy.[48,63,64] The products were purified via dialysis and lyophilization to yield white powders. As nomenclature, we adopt S70-g-OpDq to represent the graft copolymers, with S70 indicating the PSBM backbone with SBM/BIHPM as x/y =

https://dx.doi.org/10.1021/acs.macromol.0c01708
Macromolecules 2020, 53, 8267−8275

70/1, O and D representing OEGMA and DEGMA monomers, respectively, and p/q denoting the degree of degree of polymerization (DP) of the grafts. DP was determined from the monomer conversion (Figure 1 and Table 1).

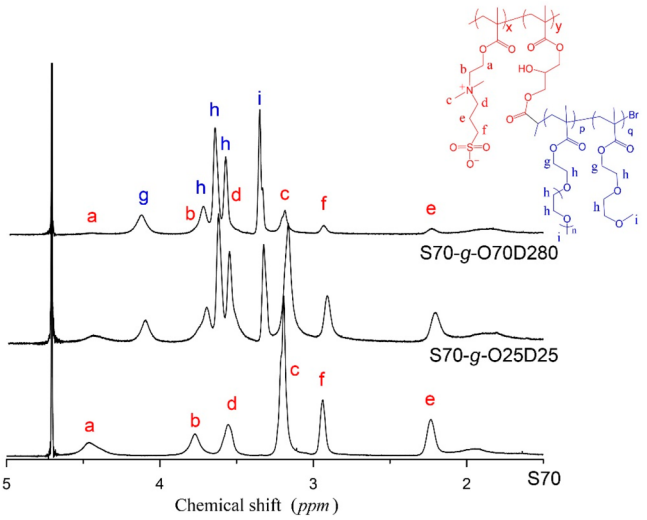

Figure 1. ^{1}H NMR spectra of the synthesized polymers S70-*g*-O25D25 and S70-*g*-O70D280 and the macroinitiator S70.

Figure 1 shows the assigned ^{1}H NMR spectra of macroinitiator S70, S70-*g*-O25D25, and S70-*g*-O70D280. Resonance peaks from O(D)EGMA side chains (marked as *g*, *h*, and *i*) can be found, indicating the presence of O(D)EGMA moieties. The integral ratio of peaks from the backbone (N-$(CH_3)_2(CH_2)_2$, marked as *c*) and side chains (*i*, resonance of proton from OCH_3) were then used to determine the DP of the side chains, which agrees well with the DP obtained from monomers conversions (Table 1).

Asymmetric flow field-flow fractionation (AF4) was used to characterize the obtained macroinitiator S70 and graft copolymers S70-*g*-O25D25 and S70-*g*-O70D280 (Figures S1–S3). AF4 shows advantages compared to SEC, especially in characterizing high-molar-mass or branched polymers.[65] Broad distributions of molecular weight were observed; see the polydispersity values in Table 1 ($Đ$, from AF4). High $Đ$ is acceptable since the macroinitiator was synthesized via free radical polymerization. In each eluogram only a single peak was observed, which together with ^{1}H NMR characterization (Figure 1) proves the successful grafting of poly(O(D)EGMA) on the macroinitiator, S70. The number-average molecular weights (M_n) of the macroinitiator S70 and the graft copolymers were 180, 248, and 616 kDa, respectively, as determined by the MALLS detector of AF4 (Table 1).

PSBM and oligo(ethylene glycol) methacrylate based polymers are well-known thermoresponsive polymers exhibiting respectively UCST[66] and LCST behavior in aqueous media. In addition, at temperatures below the cloud point of PSBM, the dissolution of the polymer can also be achieved by addition of salts (e.g., NaCl), known as salt-responsive behavior.[17] The graft copolymers S70-*g*-O25D25 and S70-*g*-O70D280 are expected to exhibit double-responsive behavior, i.e., to form core–shell and reversed nanostructures induced by respectively UCST and LCST type phase transitions in aqueous solutions. Hence, the temperature and salt-responsive and self-assembling behaviors of the obtained graft copolymers are investigated.

DLS studies were first performed by using a Malvern Zetasizer on 1 mg/mL aqueous solutions to investigate the thermoresponsive behavior of S70-*g*-O25D25 (Figure 2 and Figure S4). The intensity of the scattered light (expressed as derived rate counts of photons per second, cps) and size of the particles decrease upon heating from 5 °C. Upon further heating the size and intensity increase again at temperatures above 40 °C, indicating the formation of aggregates at both low and high temperature ranges. The size of the aggregates is ca. 30 nm above 50 °C and ca. 70 nm below 25 °C. The small particle size and weak scattering suggest relatively good thermodynamic quality of the solutions in the vicinity of 40 °C. The smallest R_h value of about 10 nm was detected at temperatures between 30 and 45 °C, which can be attributed to the coil size of the graft copolymer according to its molar mass. Such phase transition behavior can be ascribed to the LCST type phase transition of the side chains above 45 °C and the UCST type phase separation of the backbone below 30 °C. Typical size distributions for the particles are shown in Figure 2b and Figure S5. At 35 °C, a bimodal size distribution is observed with the main distribution peak at about 200 nm (intensity distribution, Figure 2b) and a main distribution peak at around 10 nm for volume distribution (Figure S5). Considering that the intensity of scattering light I is proportional to R^6, small spherical particles with $R_h \approx 10$ nm dominate in the sample, indicating the presence of mainly

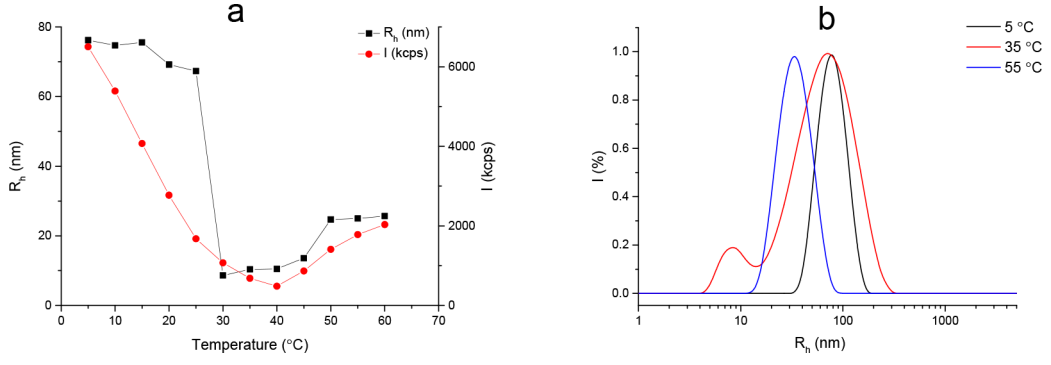

Figure 2. Dynamic light scattering data for 1 mg/mL S70-*g*-P25D25 in water. (a) Hydrodynamic size (R_h) and intensity of the scattered light (I, expressed as derived count rate in kilocounts of photons per second, kcps) versus temperature. (b) Intensity-weighed size distributions at 5, 35, and 55 °C (see also Figure S5).

https://dx.doi.org/10.1021/acs.macromol.0c01708
Macromolecules 2020, 53, 8267–8275

individual polymer chains at 35 °C. At either high or low temperatures, e.g., 55 or 5 °C, respectively, large particles are observed with quite narrow distributions (polydispersity of size estimated by DLS is ≈0.1), indicating the formation of well-defined self-assembled structures. An aqueous solution of S70-*g*-O25D25 with the presence of salt (0.1 M NaCl) was also investigated under similar conditions (see Figures S6 and S7). At high temperatures, similar aggregation process occurred, generating nanoparticles of a slightly larger size ($R_h \approx 45$ nm). No obvious changes in R_h were detected at the low temperature range even at temperatures lower than 5 °C. The nonexistence of UCST type phase transition of the saline S70-*g*-O25D25 solution below 25 °C suggests a salt responsiveness of the copolymer because of the polymer backbone.

^{1}H NMR spectra for S70-*g*-O25D25 solution in D_2O were recorded between 5 and 50 °C with an interval of 5 °C, as shown in Figure 3. At around 30 °C, all the signals of the side

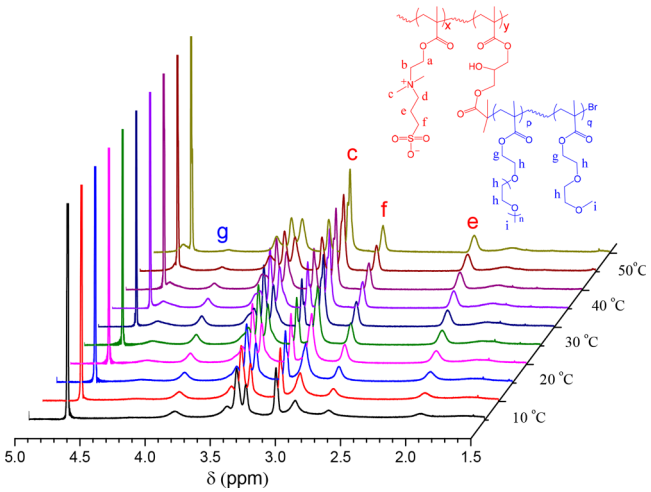

Figure 3. ^{1}H NMR spectra of S70-*g*-O25D25 in D_2O recorded between 5 and 50 °C.

chains and the backbone are clearly visible, and the integral ratios correspond to the DPs as expected for fully dissolved graft copolymers. However, characteristic resonances from the PSBM main chain (marked as *c*, *e*, and *f* in red) gradually attenuated when the temperature decreases below 20 °C. The decrease in the resonance intensity can be attributed to the restriction of the PSBM chain movement and indicates a UCST type phase separation of the backbone. In contrast, the reduction of the characteristic peak from side chains (marked as *g* in blue) at temperatures above 40 °C can be noticed, which are attributed to an LCST type phase transition of the O(D)EGMA side chains. It is worth mentioning that no significant changes of the resonance peaks from 3.0 to 3.6 ppm (assigned as *h* and *i* protons) were detected during the collapse of the side chains of the graft copolymer. Such behavior could be ascribed to a partial hydration of the oligo(ethylene glycol) chains above the critical phase transition temperature.[11] The reversing of solubility between side chain and backbone upon cooling indicates the dual-thermoresponsive character of S70-*g*-O25D25. The ^{1}H NMR spectra for S70-*g*-O25D25 solution with the presence of salt (0.1 M NaCl) are shown in Figure S8. A similar decrease of the signal from *g* protons was observed, indicating the LCST type phase transition of the side chains. However, no significant changes in the intensities of the PSBM backbone resonance signals were observed at low temperatures, indicating the loss of the UCST transition for PSBM in saline solution.

To further investigate the structure of the obtained self-assembled nanoaggregates, transmission electron microscopy-(TEM) and cryo-TEM were performed under selected conditions. Unfortunately, neither TEM nor cryo-TEM was able to detect the nanostructures of the system, which might be due to the low density and thus insufficient contrast of the polymers.[67]

Further LS measurements on the aqueous polymers were performed on a Brookhaven instrument to give both the hydrodynamic radius (R_h) and the radius of gyration (R_g) of the self-assembled nanoparticles (Figure 4, Figure S9, and Table 2). The ratio of R_g over R_h ($\rho = R_g/R_h$) was calculated as an indicator of the architecture of the studied nanoparticles.[68] In general, values of ρ = 0.7, 1.0, 1.7, and >2.0 correspond to a hard sphere, a vesicle, a cylinder, and a rod, respectively.[69] The R_h of S70-*g*-O25D25 at 50 °C in water was 29.8 nm, which is in good accordance with the result obtained with the Malvern instrument. The SLS data were evaluated with three models, namely Zimm, Guinier, and Debye−Bueche. The first-order Zimm fit was the best one, leading to a radius of gyration R_g = 33.4 nm. Hence, the ρ value for S70-*g*-O25D25 assembly at 50 °C is 1.12. Although this ρ value is close to the value of a typical vesicle, the structure of the studied particles cannot be a vesicle due to two reasons. First, the hydrophobic/hydrophilic ratio of the copolymer is too low to form vesicles. The hydrophobic/hydrophilic ratio (in volume) is one of the main facts that determines the self-assembly structure of copolymers; i.e., with the increasing of hydrophobic/hydrophilic ratio of the copolymer, its self-assembling structure usually undergoes a change from spherical micelles to elongated micelles and to vesicles. As for S70-*g*-O70D280 with a much higher hydrophobic/hydrophilic ratio, only micelles were formed (stated in the next section); also, the nanoparticles of S70-*g*-O25D25 should be micelles. Second, the size distributions of vesicles are usually broad, while the studied nanoparticles have low polydispersity (~0.1) by DLS. Hence, we assume a loose multimolecular aggregate (LMMA) forms with a shell of PSBM backbone chains and a water-swollen core of PO(D)-EGMA chains. In 0.1 M NaCl at 50 °C, S70-*g*-O25D25 gave a ρ value of 0.76 (R_h = 44.9 nm, R_g = 34.2 nm), indicating the formation of micelles. Such a change on the packing of polymer chains can be ascribed to the increasing of hydrophobicity of PO(D)EGMA core because of the salting out effect by NaCl. Below the UCST type phase transition temperature, 15 °C, R_h and R_g were 67.6 nm and 72.4 nm, respectively, leading to a ρ value of 1.07. The structure of the particles was also proposed to be LMMA due to the same reasons as in the case of 50 °C.

The S70-*g*-O70D280 was also investigated by SLS. The difference between the two polymers lies on the higher DP and higher DEGMA content of the side chains for S70-*g*-O70D280. DLS of S70-*g*-O70D280 in water at 50 °C (Figure 5 and Figure S10) showed an R_h around 50 nm and a narrow size distribution (polydispersity <0.1), similarly as observed at high temperature for S70-*g*-O25D25. The decrease of size and scattering intensity were also evidenced upon cooling but with a lower transition temperature (30−35 °C) than for S70-*g*-O25D25 solutions (45−50 °C) due to the higher content of the less hydrophilic DEGMA component. The LCST type phase transition was also evidenced by ^{1}H NMR with D_2O as

https://dx.doi.org/10.1021/acs.macromol.0c01708
Macromolecules 2020, 53, 8267−8275

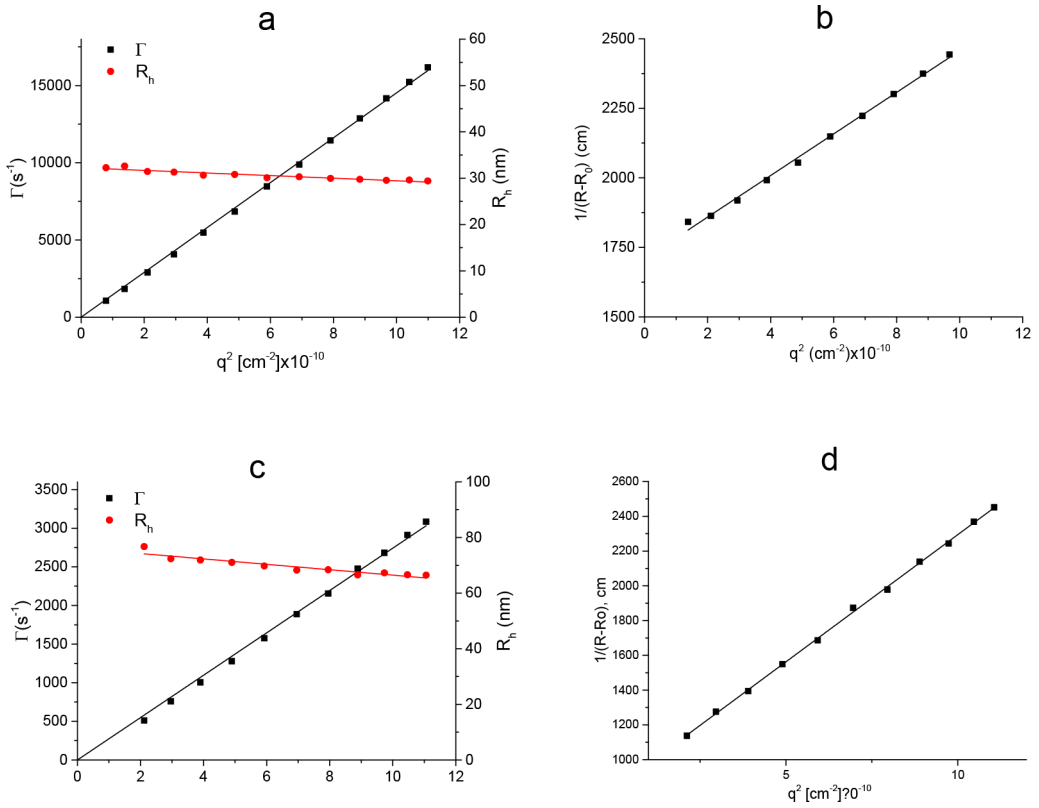

Figure 4. Hydrodynamic radius (R_h), relaxation rate (Γ), and intensity of the scattered light expressed as the excess Rayleigh ratio ($R - R_0$) versus scattering vector (q) for S70-*g*-O25P25 in aqueous solution (a) at 50 and (c) 15 °C. Debye plot for S70-D25P25 in aqueous solution (b) at 50 and (d) 15 °C; all the data are collected for S70-D25P25aqueous solution with the absence of salt, at a concentration of 1 mg/mL.

Table 2. Summary of Light Scattering Data for S70-*g*-O25D25 and S70-*g*-O70D280 under Various Conditions

	S70-*g*-O25D25			S70-*g*-O70D280	
	50 °C, water	50 °C, 0.1 M NaCl	15 °C, water	50 °C, water	50 °C, 0.1 M NaCl
R_h (nm)	29.8	44.9	67.6	47.0	60.4
R_g (nm)	33.4	34.2	72.4	32.8	39.4
R_g/R_h	1.12	0.76	1.07	0.70	0.65

solvent (Figure 6 and Figure S11). The R_h, R_g, and ρ values for S70-*g*-O70D280 at 50 °C in aqueous solution with and without 0.1 M NaCl were determined by using SLS and DLS (Table 2 and Figures S12 and S13). Larger particle sizes than for S70-*g*-O25D25 were obtained, and the ρ values (0.7 in water and 0.65 in 0.1 M NaCl) indicate micelle-like aggregates with side chains situated mainly in the core and the PBMA backbone forming the shell.

In contrast to S70-*g*-O25D25, the size of the S70-*g*-O70D280 particles did not increase upon cooling to 5 °C in water. Instead, the size of the nanoparticles slightly decreased and the intensity of scattered light kept nearly constant upon cooling. This suggests that most of the individual macromolecules do not associate below the LCST type phase transition temperature. Yet, the question remains whether the intramolecular self-assembling is due to the UCST type phase transition of the PSBM backbone or not. ^{1}H NMR spectra for the aqueous polymer solution were therefore collected at various temperatures (Figure 6). Characteristic signals from the PSBM main chain (*c*, *e*, and *f*, marked in red), which were visible with reasonable resolution at temperatures above 25 °C, diminished when the temperature decreased to 20 °C and

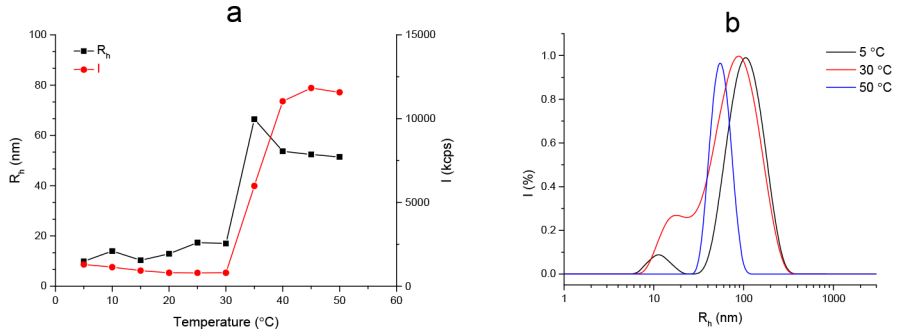

Figure 5. Dynamic light scattering data for 1 mg/mL S70-*g*-P70D280 in water. (a) Hydrodynamic size (R_h) and intensity of the scattered light (I) versus temperature. (b) Intensity-weighted size distribution at 5, 35, and 55 °C.

https://dx.doi.org/10.1021/acs.macromol.0c01708
Macromolecules 2020, 53, 8267−8275

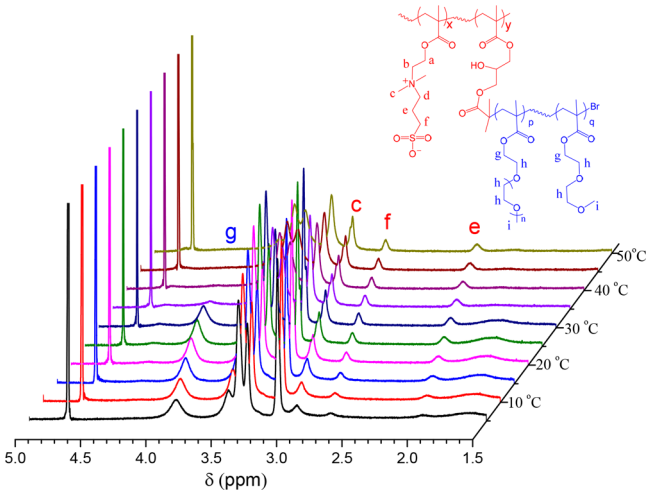

Figure 6. ^{1}H NMR spectra for S70-*g*-O70D280 in D_2O without salt at various temperatures.

lower. The decrease in the signal intensity indicates a UCST type phase separation of the PSBM backbone as is the case of S70-*g*-O25D25 and, thus, together with LS results suggests the formation of small micelles with a low aggregation number. To further investigate the self-assembly of S70-*g*-O70D280 below the UCST type phase separation temperature, comparison of the ^{1}H NMR spectra collected at 5 °C with and without the presence of 0.1 M NaCl was made as shown in Figure S14. The attenuation of the proton signals from PSBM without salt could be clearly observed in comparison with the spectrum with salt, in which case the PSBM backbone is permanently soluble. The difference confirms the UCST type phase transition of the copolymer in water at 5 °C. SLS measurement was then performed at temperature below (15 °C) and above the phase transition temperature (25 °C) of S70-*g*-P70D280. A partial Zimm model was applied to calculate apparent ($M_{w,app}$) values at both temperatures. The aggregation number N_{agg} was estimated accordingly to be 2.2, which is in good agreement with the previous DLS result.

The low aggregation number for S70-*g*-O70D280 in aqueous solution can be rationalized by its topology. S70-*g*-O70D280 is characterized by its long and loose side chains as well as high molecular weight. Upon the phase separation of the PSBM backbone and formation of the micelles, the soluble side chains can restrict the aggregation of the polymers due to the steric effect. Such result is consistent with previously reported unimolecular micelles of a graft copolymer with a high graft density.[49,50,52]

CONCLUSIONS

Two graft copolymers, S70-*g*-O25D25 and S70-*g*-O70D280, with PSBM backbone showing UCST behavior and PO(D)EGMA side chains with LCST behavior were prepared and investigated by using DLS, SLS, AF4, and ^{1}H NMR. The graft copolymers were found to undergo both UCST and LCST type phase transitions and are capable to form various self-assembled structures depending on temperature and the ionic strength. At low temperatures in water aggregates with PSBM cores form due to the PSBM UCST type phase transition. The increasing volume of the side chains in the case of S70-*g*-O70D280 leads to micelles with PSBM core and PO(D)EGMA shell with extremely low aggregation number. Upon heating the aggregates of both polymers break and dissolve to soluble unimers until the LCST type phase transition temperature is reached. Above the LCST type phase transition reverse aggregates with O(D)EGMA cores are formed, and the phase transition temperature changes depending on OEGMA/DEGMA ratio of the grafts. In 0.1 M NaCl the UCST transition of PSBM disappears for both polymers, demonstrating their salt-responsive behavior. Moreover, the increased ionic strength also affects the structure of the micelles, leading to closer packing of the PO(D)EGMA chains at elevated temperatures. The adjustable self-assembling behavior of the graft copolymer is of great interest for application in smart materials such as drug delivery polymers or sensors.[70,71]

ASSOCIATED CONTENT

Supporting Information

The Supporting Information is available free of charge at https://pubs.acs.org/doi/10.1021/acs.macromol.0c01708.

AF4 eluograms, light scattering data, and NMR spectra of the polymers (PDF)

AUTHOR INFORMATION

Corresponding Authors

Qilu Zhang − *Department of Chemistry, University of Helsinki, 00014 Helsinki, Finland; State Key Laboratory for Mechanical Behavior of Materials, Xi'an Jiaotong University, Xi'an 710049, China;* orcid.org/0000-0001-5706-9250; Email: qilu.zhang@xjtu.edu.cn

Heikki Tenhu − *Department of Chemistry, University of Helsinki, 00014 Helsinki, Finland;* orcid.org/0000-0001-5957-4541; Email: heikki.tenhu@helsinki.fi

Authors

Tao Jiang − *Department of Chemistry, University of Helsinki, 00014 Helsinki, Finland*

Vladimir Aseyev − *Department of Chemistry, University of Helsinki, 00014 Helsinki, Finland;* orcid.org/0000-0002-3739-8089

Jukka Niskanen − *Department of Chemistry, University of Helsinki, 00014 Helsinki, Finland; Department of Chemical and Biological Engineering, University of Ottawa, Ottawa, ON, Canada K1N 6N5;* orcid.org/0000-0002-7001-7129

Sami Hietala − *Department of Chemistry, University of Helsinki, 00014 Helsinki, Finland;* orcid.org/0000-0003-1448-1813

Complete contact information is available at: https://pubs.acs.org/10.1021/acs.macromol.0c01708

Notes

The authors declare no competing financial interest.

REFERENCES

(1) Löwenberg, C.; Balk, M.; Wischke, C.; Behl, M.; Lendlein, A. Shape-Memory Hydrogels: Evolution of Structural Principles To Enable Shape Switching of Hydrophilic Polymer Networks. *Acc. Chem. Res.* **2017**, *50*, 723−732.

(2) Zhang, Q.; Weber, C.; Schubert, U. S.; Hoogenboom, R. Thermoresponsive Polymers with Lower Critical Solution Temperature: From Fundamental Aspects and Measuring Techniques to Recommended Turbidimetry Conditions. *Mater. Horiz.* **2017**, *4*, 109−116.

(3) Lu, W.; Le, X.; Zhang, J.; Huang, Y.; Chen, T. Supramolecular Shape Memory Hydrogels: A New Bridge between Stimuli-

Responsive Polymers and Supramolecular Chemistry. *Chem. Soc. Rev.* **2017**, *46*, 1284−1294.
(4) Zhao, Q.; Qi, H. J.; Xie, T. Recent Progress in Shape Memory Polymer: New Behavior, Enabling Materials, and Mechanistic Understanding. *Prog. Polym. Sci.* **2015**, *49*−*50*, 79−120.
(5) Zhu, Y.; Yang, B.; Chen, S.; Du, J. Polymer Vesicles: Mechanism, Preparation, Application, and Responsive Behavior. *Prog. Polym. Sci.* **2017**, *64*, 1−22.
(6) Deng, R.; Derry, M. J.; Mable, C. J.; Ning, Y.; Armes, S. P. Using Dynamic Covalent Chemistry to Drive Morphological Transitions: Controlled Release of Encapsulated Nanoparticles from Block Copolymer Vesicles. *J. Am. Chem. Soc.* **2017**, *139*, 7616−7623.
(7) Hu, X.; Zhai, S.; Liu, G.; Xing, D.; Liang, H.; Liu, S. Concurrent Drug Unplugging and Permeabilization of Polyprodrug-Gated Cross-linked Vesicles for Cancer Combination Chemotherapy. *Adv. Mater.* **2018**, *30*, 1−7.
(8) Zhang, Q.; Vanparijs, N.; Louage, B.; De Geest, B. G.; Hoogenboom, R. Dual PH- and Temperature-Responsive RAFT-Based Block Co-Polymer Micelles and Polymer-Protein Conjugates with Transient Solubility. *Polym. Chem.* **2014**, *5*, 1140−1144.
(9) Bütün, V.; Billingham, N. C.; Armes, S. P. Unusual Aggregation Behavior of a Novel Tertiary Amine Methacrylate-Based Diblock Copolymer: Formation of Micelles and Reverse Micelles in Aqueous Solution. *J. Am. Chem. Soc.* **1998**, *120*, 11818−11819.
(10) Liu, S.; Billingham, N. C.; Armes, S. P. A Schizophrenic Water-Soluble Diblock Copolymer. *Angew. Chem., Int. Ed.* **2001**, *40*, 2328−2331.
(11) Zhang, Q.; Hong, J.-D.; Hoogenboom, R. A Triple Thermoresponsive Schizophrenic Diblock Copolymer. *Polym. Chem.* **2013**, *4*, 4322−4325.
(12) Feng, A.; Zhan, C.; Yan, Q.; Liu, B.; Yuan, J. A CO_2- and Temperature-Switchable "Schizophrenic" Block Copolymer: From Vesicles to Micelles. *Chem. Commun.* **2014**, *50*, 8958−8961.
(13) Zhou, Y.-N.; Zhang, Q.; Luo, Z.-H. A Light and pH Dual-Stimuli-Responsive Block Copolymer Synthesized by Copper(0)-Mediated Living Radical Polymerization: Solvatochromic, Isomerization, and "Schizophrenic" Behaviors. *Langmuir* **2014**, *30*, 1489−1499.
(14) Vasantha, V. A.; Jana, S.; Lee, S. S.-C.; Lim, C.-S.; Teo, S. L.-M.; Parthiban, A.; Vancso, J. G. Dual Hydrophilic and Salt Responsive Schizophrenic Block Copolymers − Synthesis and Study of Self-Assembly Behavior. *Polym. Chem.* **2015**, *6*, 599−606.
(15) Bütün, V.; Liu, S.; Weaver, J. V. M.; Bories-Azeau, X.; Cai, Y.; Armes, S. P. A Brief Review of 'Schizophrenic' Block Copolymers. *React. Funct. Polym.* **2006**, *66*, 157−165.
(16) Hildebrand, V.; Heydenreich, M.; Laschewsky, A.; Möller, H. M.; Müller-Buschbaum, P.; Papadakis, C. M.; Schanzenbach, D.; Wischerhoff, E. Schizophrenic" Self-Assembly of Dual Thermoresponsive Block Copolymers Bearing a Zwitterionic and a Non-Ionic Hydrophilic Block. *Polymer* **2017**, *122*, 347−357.
(17) Virtanen, J.; Arotçaréna, M.; Heise, B.; Ishaya, S.; Laschewsky, A.; Tenhu, H. Dissolution and Aggregation of a Poly(NIPA- Block -Sulfobetaine) Copolymer in Water and Saline Aqueous Solutions. *Langmuir* **2002**, *18*, 5360−5365.
(18) Liu, S.; Armes, S. P. Polymeric Surfactants for the New Millennium: A PH-Responsive, Zwitterionic, Schizophrenic Diblock Copolymer. *Angew. Chem., Int. Ed.* **2002**, *41*, 1413−1416.
(19) Arotçaréna, M.; Heise, B.; Ishaya, S.; Laschewsky, A. Switching the Inside and the Outside of Aggregates of Water-Soluble Block Copolymers with Double Thermoresponsivity. *J. Am. Chem. Soc.* **2002**, *124*, 3787−3793.
(20) Cai, Y.; Armes, S. P. A Zwitterionic ABC Triblock Copolymer That Forms a "Trinity" of Micellar Aggregates in Aqueous Solution. *Macromolecules* **2004**, *37*, 7116−7122.
(21) Ge, Z.; Cai, Y.; Yin, J.; Zhu, Z.; Rao, J.; Liu, S. Synthesis and 'Schizophrenic" Micellization of Double Hydrophilic AB 4 Miktoarm Star and AB Diblock Copolymers: Structure and Kinetics of Micellization. *Langmuir* **2007**, *23*, 1114−1122.
(22) Rao, J.; Luo, Z.; Ge, Z.; Liu, H.; Liu, S. Schizophrenic" Micellization Associated with Coil-to-Helix Transitions Based on Polypeptide Hybrid Double Hydrophilic Rod−Coil Diblock Copolymer. *Biomacromolecules* **2007**, *8*, 3871−3878.
(23) Chang, C.; Wei, H.; Feng, J.; Wang, Z.-C.; Wu, X.-J.; Wu, D.-Q.; Cheng, S.-X.; Zhang, X.-Z.; Zhuo, R.-X. Temperature and pH Double Responsive Hybrid Cross-Linked Micelles Based on P-(NIPAAm- Co -MPMA)- b -P(DEA): RAFT Synthesis and "Schizophrenic" Micellization. *Macromolecules* **2009**, *42*, 4838−4844.
(24) Du, J.; O'Reilly, R. K. pH-Responsive Vesicles from a Schizophrenic Diblock Copolymer. *Macromol. Chem. Phys.* **2010**, *211*, 1530−1537.
(25) Shih, Y.-J.; Chang, Y.; Deratani, A.; Quemener, D. Schizophrenic" Hemocompatible Copolymers via Switchable Thermoresponsive Transition of Nonionic/Zwitterionic Block Self-Assembly in Human Blood. *Biomacromolecules* **2012**, *13*, 2849−2858.
(26) Yin, J.; Hu, J.; Zhang, G.; Liu, S. Schizophrenic Core-Shell Microgels: Thermoregulated Core and Shell Swelling/Collapse by Combining UCST and LCST Phase Transitions. *Langmuir* **2014**, *30*, 2551−2558.
(27) Mäkinen, L.; Varadharajan, D.; Tenhu, H.; Hietala, S. Triple Hydrophilic UCST-LCST Block Copolymers. *Macromolecules* **2016**, *49*, 986−993.
(28) Weaver, J. V. M.; Armes, S. P.; Bütün, V. Synthesis and Aqueous Solution Properties of a Well-Defined Thermo-Responsive Schizophrenic Diblock Copolymer. *Chem. Commun.* **2002**, 2122−2123.
(29) Maeda, Y.; Mochiduki, H.; Ikeda, I. Hydration Changes during Thermosensitive Association of a Block Copolymer Consisting of LCST and UCST Blocks. *Macromol. Rapid Commun.* **2004**, *25*, 1330−1334.
(30) Vishnevetskaya, N. S.; Hildebrand, V.; Niebuur, B.-J.; Grillo, I.; Filippov, S. K.; Laschewsky, A.; Müller-Buschbaum, P.; Papadakis, C. M. Aggregation Behavior of Doubly Thermoresponsive Polysulfobetaine-b-Poly(N-Isopropylacrylamide) Diblock Copolymers. *Macromolecules* **2016**, *49*, 6655−6668.
(31) Vishnevetskaya, N. S.; Hildebrand, V.; Niebuur, B. J.; Grillo, I.; Filippov, S. K.; Laschewsky, A.; Müller-Buschbaum, P.; Papadakis, C. M. Schizophrenic" Micelles from Doubly Thermoresponsive Polysulfobetaine-b-Poly(N-Isopropylmethacrylamide) Diblock Copolymers. *Macromolecules* **2017**, *50*, 3985−3999.
(32) Vishnevetskaya, N. S.; Hildebrand, V.; Dyakonova, M. A.; Niebuur, B. J.; Kyriakos, K.; Raftopoulos, K. N.; Di, Z.; Müller-Buschbaum, P.; Laschewsky, A.; Papadakis, C. M. Dual Orthogonal Switching of the "Schizophrenic" Self-Assembly of Diblock Copolymers. *Macromolecules* **2018**, *51*, 2604−2614.
(33) Plamper, F. A.; Schmalz, A.; Ballauff, M.; Müller, A. H. E. Tuning the Thermoresponsiveness of Weak Polyelectrolytes by PH and Light: Lower and Upper Critical-Solution Temperature of Poly(N,N-Dimethylaminoethyl Methacrylate). *J. Am. Chem. Soc.* **2007**, *129*, 14538−14539.
(34) Zhang, Q.; Tosi, F.; Üğdüler, S.; Maji, S.; Hoogenboom, R. Tuning the LCST and UCST Thermoresponsive Behavior of Poly(N,N -Dimethylaminoethyl Methacrylate) by Electrostatic Interactions with Trivalent Metal Hexacyano Anions and Copolymerization. *Macromol. Rapid Commun.* **2015**, *36*, 633−639.
(35) Tyrrell, Z. L.; Shen, Y.; Radosz, M. Fabrication of Micellar Nanoparticles for Drug Delivery through the Self-Assembly of Block Copolymers. *Prog. Polym. Sci.* **2010**, *35*, 1128−1143.
(36) Gaitzsch, J.; Appelhans, D.; Wang, L.; Battaglia, G.; Voit, B. Synthetic Bio-Nanoreactor: Mechanical and Chemical Control of Polymersome Membrane Permeability. *Angew. Chem., Int. Ed.* **2012**, *51*, 4448−4451.
(37) Yan, X.; Wang, F.; Zheng, B.; Huang, F. Stimuli-Responsive Supramolecular Polymeric Materials. *Chem. Soc. Rev.* **2012**, *41*, 6042.
(38) Ji, X.; Dong, S.; Wei, P.; Xia, D.; Huang, F. A Novel Diblock Copolymer with a Supramolecular Polymer Block and a Traditional Polymer Block: Preparation, Controllable Self-Assembly in Water, and Application in Controlled Release. *Adv. Mater.* **2013**, *25*, 5725−5729.

https://dx.doi.org/10.1021/acs.macromol.0c01708
Macromolecules 2020, 53, 8267−8275

(39) Jabbarzadeh, A.; Atkinson, J. D.; Tanner, R. I. Effect of Molecular Shape on Rheological Properties in Molecular Dynamics Simulation of Star, H, Comb, and Linear Polymer Melts. *Macromolecules* **2003**, *36*, 5020−5031.
(40) Cai, Y.; Tang, Y.; Armes, S. P. Direct Synthesis and Stimulus-Responsive Micellization of Y-Shaped Hydrophilic Block Copolymers. *Macromolecules* **2004**, *37*, 9728−9737.
(41) Cai, Y.; Armes, S. P. Synthesis of Well-Defined Y-Shaped Zwitterionic Block Copolymers via Atom-Transfer Radical Polymerization. *Macromolecules* **2005**, *38*, 271−279.
(42) Tezuka, Y.; Oike, H. Topological Polymer Chemistry: Systematic Classification of Nonlinear Polymer Topologies. *J. Am. Chem. Soc.* **2001**, *123*, 11570−11576.
(43) Hadjichristidis, N.; Pitsikalis, M.; Pispas, S.; Iatrou, H. Polymers with Complex Architecture by Living Anionic Polymerization. *Chem. Rev.* **2001**, *101*, 3747−3792.
(44) McKee, M. G.; Unal, S.; Wilkes, G. L.; Long, T. E. Branched Polyesters: Recent Advances in Synthesis and Performance. *Prog. Polym. Sci.* **2005**, *30*, 507−539.
(45) Sheiko, S. S.; Sumerlin, B. S.; Matyjaszewski, K. Cylindrical Molecular Brushes: Synthesis, Characterization, and Properties. *Prog. Polym. Sci.* **2008**, *33*, 759−785.
(46) Lee, H.; Pietrasik, J.; Sheiko, S. S.; Matyjaszewski, K. Stimuli-Responsive Molecular Brushes. *Prog. Polym. Sci.* **2010**, *35*, 24−44.
(47) Zhang, M.; Müller, A. H. E. Cylindrical Polymer Brushes. *J. Polym. Sci., Part A: Polym. Chem.* **2005**, *43*, 3461−3481.
(48) Feng, C.; Li, Y.; Yang, D.; Hu, J.; Zhang, X.; Huang, X. Well-Defined Graft Copolymers: From Controlled Synthesis to Multipurpose Applications. *Chem. Soc. Rev.* **2011**, *40*, 1282−1295.
(49) Tuzar, Z.; Kratochvíl, P. Block and Graft Copolymer Micelles in Solution. *Adv. Colloid Interface Sci.* **1976**, *6*, 201−232.
(50) Pispas, S.; Hadjichristidis, N.; Mays, J. W. Micellization of Model Graft Copolymers of the H and π Type in Dilute Solution. *Macromolecules* **1996**, *29* (23), 7378−7385.
(51) Borisov, O. V.; Zhulina, E. B. Amphiphilic Graft Copolymer in a Selective Solvent: Intramolecular Structures and Conformational Transitions. *Macromolecules* **2005**, *38*, 2506−2514.
(52) Štěpánek, M.; KoŠovan, P.; Procházka, K.; Janata, M.; Netopilík, M.; PleŠtil, J.; Šlouf, M. Self-Assembly of Poly(4-Methylstyrene)- g -Poly(Methacrylic Acid) Graft Copolymer in Selective Solvents for Grafts: Scattering and Molecular Dynamics Simulation Study. *Langmuir* **2010**, *26*, 9289−9296.
(53) Jiang, X.; Lu, G.; Feng, C.; Li, Y.; Huang, X. Poly(Acrylic Acid)-Graft-Poly(N-Vinylcaprolactam): A Novel PH and Thermo Dual-Stimuli Responsive System. *Polym. Chem.* **2013**, *4*, 3876.
(54) Williams, R. J.; Pitto-Barry, A.; Kirby, N.; Dove, A. P.; O'Reilly, R. K. Cyclic Graft Copolymer Unimolecular Micelles: Effects of Cyclization on Particle Morphology and Thermoresponsive Behavior. *Macromolecules* **2016**, *49*, 2802−2813.
(55) Fan, X.; Li, Z.; Loh, X. J. Recent Development of Unimolecular Micelles as Functional Materials and Applications. *Polym. Chem.* **2016**, *7*, 5898−5919.
(56) Chan, D.; Yu, A. C.; Appel, E. A. Single-Chain Polymeric Nanocarriers: A Platform for Determining Structure-Function Correlations in the Delivery of Molecular Cargo. *Biomacromolecules* **2017**, *18*, 1434−1439.
(57) Muljajew, I.; Weber, C.; Nischang, I.; Schubert, U. PMMA-g-OEtOx Graft Copolymers: Influence of Grafting Degree and Side Chain Length on the Conformation in Aqueous Solution. *Materials* **2018**, *11*, 528.
(58) Zhang, H.; Wu, W.; Zhao, X.; Zhao, Y. Synthesis and Thermoresponsive Behaviors of Thermo-, PH-, CO_2-, and Oxidation-Responsive Linear and Cyclic Graft Copolymers. *Macromolecules* **2017**, *50*, 3411−3423.
(59) Percec, V.; Guliashvili, T.; Ladislaw, J. S.; Wistrand, A.; Stjerndahl, A.; Sienkowska, M. J.; Monteiro, M. J.; Sahoo, S. Ultrafast Synthesis of Ultrahigh Molar Mass Polymers by Metal-Catalyzed Living Radical Polymerization of Acrylates, Methacrylates, and Vinyl Chloride Mediated by SET at 25 °C. *J. Am. Chem. Soc.* **2006**, *128*, 14156−14165.
(60) Voorhaar, L.; Wallyn, S.; Du Prez, F. E.; Hoogenboom, R. Cu(0)-Mediated Polymerization of Hydrophobic Acrylates Using High-Throughput Experimentation. *Polym. Chem.* **2014**, *5*, 4268−4276.
(61) Rosen, B. M.; Percec, V. Single-Electron Transfer and Single-Electron Transfer Degenerative Chain Transfer Living Radical Polymerization. *Chem. Rev.* **2009**, *109*, 5069−5119.
(62) Vancoillie, G.; Frank, D.; Hoogenboom, R. Thermoresponsive Poly(Oligo Ethylene Glycol Acrylates). *Prog. Polym. Sci.* **2014**, *39*, 1074−1095.
(63) Borner, H. G.; Beers, K.; Matyjaszewski, K.; Sheiko, S. S.; Möller, M. Synthesis of Molecular Brushes with Block Copolymer Side Chains Using Atom Transfer Radical Polymerization. *Macromolecules* **2001**, *34*, 4375−4383.
(64) Beers, K. L.; Gaynor, S. G.; Matyjaszewski, K.; Sheiko, S. S.; Moeller, M. Synthesis of Densely Grafted Copolymers by Atom Transfer Radical Polymerization. *Macromolecules* **1998**, *31*, 9413−9415.
(65) Podzimek, S. Asymmetric Flow Field Flow Fractionation. In *Light Scattering, Size Exclusion Chromatography and Asymmetric Flow Field Flow Fractionation*; 2011; pp 259−305.
(66) Seuring, J.; Agarwal, S. Polymers with Upper Critical Solution Temperature in Aqueous Solution. *Macromol. Rapid Commun.* **2012**, *33*, 1898−1920.
(67) Zhang, Q.; Voorhaar, L.; Filippov, S. K.; Yeşil, B. F.; Hoogenboom, R. Tuning of Polymeric Nanoparticles by Coassembly of Thermoresponsive Polymers and a Double Hydrophilic Thermoresponsive Block Copolymer. *J. Phys. Chem. B* **2016**, *120*, 4635−4643.
(68) Burchard, W. Static and Dynamic Light Scattering from Branched Polymers and Biopolymers. *Adv. Polym. Sci.* **1983**, *48*, 1−124.
(69) Burchard, W.; Richtering, W. Dynamic Light Scattering from Polymer Solutions. In *Relaxation in Polymers*; Pietralla, M., Pechhold, W., Eds.; Steinkopff: Darmstadt, 1989; pp 151−163.
(70) Zhang, J.; Xiao, Y.; Luo, X.; Wen, L.; Heise, A.; Lang, M. Schizophrenic Poly(ϵ-Caprolactone)s Synthesis, Self-Assembly and Fluorescent Decoration. *Polym. Chem.* **2017**, *8*, 3261−3270.
(71) Grubbs, R. B.; Sun, Z. Shape-Changing Polymer Assemblies. *Chem. Soc. Rev.* **2013**, *42*, 7436−7445.

https://dx.doi.org/10.1021/acs.macromol.0c01708
Macromolecules 2020, 53, 8267−8275